AKADÉMIAI KIADÓ

UNIVERSITY of DEBRECEN

International Review of Applied Sciences and Engineering

14 (2023) 3, 316–324

DOI:
10.1556/1848.2023.00546

ORIGINAL RESEARCH PAPER

A novel approach of multi-loop control based-ADRC for improving lower knee position exoskeleton system

Nasir Ahmed Alawad[1,2*], Amjad Jaleel Humaidi[2] and Ahmed Sabah Alaraji[3]

[1] Department of Computer Engineering, Faculty of Engineering, Mustansiriyah University, Baghdad, Iraq

[2] Control and Systems Engineering Department, University of Technology, Baghdad, Iraq

[3] Department of Computer Engineering, University of Technology, Baghdad, Iraq

Received: October 8, 2022 • Accepted: January 16, 2023
Published online: March 9, 2023

ABSTRACT

This study revealed the system of a lower limb exoskeleton created for knee rehabilitation. The exoskeleton has been extensively used in rehabilitation robotic device research, but its practical applicability is limited due to its high nonlinearity and uncertain behavior. As a result, the control technique is critical in increasing the efficacy of rehabilitation devices. For the rehabilitation and help of a patient with a lower-limb condition, a sliding mode control (SMC) with proportional derivative (PD) control approach are used as parallel loops. Active disturbances rejection control (ADRC) is used by these controllers to cancel any external influences. To overcome the degradation of disturbance rejection and robustness caused by a failure to fully adjust for the entire disturbance, a (SMC) loop was introduced to the control regulation. By assessing performance indices related to the estimated inaccuracy, the results demonstrate the effectiveness of the suggested controller. Simulink is used for simulation and analysis.

KEYWORDS

lower extremity, ADRC, SMC, PD controller, trajectory tracking, exogenous disturbances

1. INTRODUCTION

Exoskeletons are a type of mechanical robot that can help people and improve their physical capabilities, such as enhancing soldier strength, supporting the elderly in walking, and healing patients with limb injuries. It has attracted a lot of attention in recent years [1, 2]. The lower leg is the weakest of the limb joints in humans. It facilitates in human movement by supporting body weight, absorbing impact stress, and assisting lower limb swing [3]. Over the past few decades, different control techniques have been researched to increase the accuracy of joint motion control for exoskeletons. In [4, 5] used a feedback and feed forward proportional–integral–derivative (PID) controller for monitoring the limb exoskeleton's desirable output. Despite its ease of implementation, the usage of PID control is limited by the convergence analysis and coefficients adjustment. Soft computing approaches such as fuzzy sets and artificial neural networks have been investigated in recent years (ANNs). For exoskeletons, a fuzzy controller with a bang-bang controller has been proposed [6]. In [7] the rehabilitation robot developed an adaptive self-organizing fuzzy controller. In [8] it was demonstrated how to achieve accurate control performance using ANN-based model predictive control (MPC) methods. Despite the ability to approximate nonlinear properties, real-time performance is constrained, and all of these control applications are limited. System uncertainties,

*Corresponding author.
E-mail: cse.20.33@grad.uotechnology.edu.iq

such as exogenous disruptions, unmodeled dynamics, and parameter perturbations, have a significant impact on the performance of a control system. The development of the any controller that attempts to fulfill these objectives while also assuring disturbance rejection and strong tracking performance in the face of huge uncertainty is complicated. As a result, anti-disturbance approaches using both external- and internal-loop controllers and estimators have been widely employed [9]. The ADRC controller was first proposed in [10], which offers many benefits. The industry's rapid adoption of ADRC over the past three decades is evidence of the technology's value in position control and other application fields [11–15]. Regarding the biomechanics of the exoskeleton, (SMC) may be an appropriate solution due to its robustness to both internal and external system uncertainties [16–18]. To achieve optimal performance, SMC parameters should be chosen carefully. Genetic Algorithm GA [19], particle swarm optimization (PSO) [20], and Grey-wolf optimization [21] are examples of common optimization methods that are given and used in exoskeleton devices. Algorithm for ant colony optimization [22] was also used. GA is easy to use and capable of finding global optima, which can be used to improve the structure of optimization systems [23]. In this research, a hybrid proposed control technique that combines optimal SMC and PD compensation is presented.

The contributions of this study can be highlighted by the following points:

- This study has proposed an expanded ADRC by adding a second SMC-LESO in combination with a PD controller LESO to produce a multilayered LESO. It is particularly efficient to use numerous LESOs within that ADRC framework when dealing with highly unpredictable nonlinear systems.
- The controlled system's stability and global convergence properties have been verified according to Lyapunov's second approach
- By choosing the best gains for the observer and sliding surface of the SMC technique the chattering phenomenon is minimized.

The rest of this paper is laid out as follows. In the second part, the particular human exoskeleton under investigation is described. The proposed control strategy is clearly described in Section 3. The fourth part incorporates simulations and analysis of results utilizing the proposed approach. In the concluding section, conclusions are formed.

2. EXOSKELETON MATHEMATICAL REPRESENTATION

Figure 1 illustrates how the grouped human-exoskeleton model is realized as a rigid body system represented by a kinematic plant with the objective of studying the dynamical behavior of the human-exoskeleton system without overhyping by taking into account the flexible components included in the patient's psyche and mechanical linkages. A numerical equation of the dynamics of the system depending on the inertia concept can be created using Euler-Lagrangian equations of rigid body dynamics. For helping knee flexion and extension workouts, it designed a stationary 1-DOF exoskeleton as [8, 14, 24, 25]

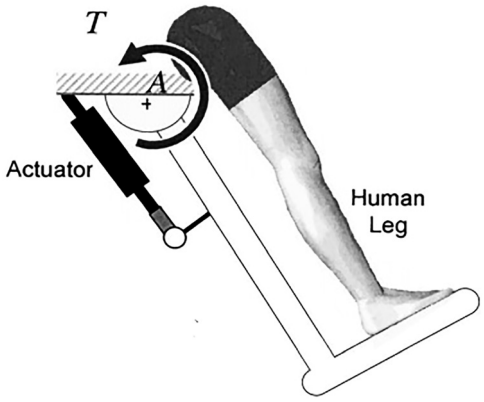

Fig. 1. Simple 1-DOF exoskeleton leg

$$J\ddot{\theta} = -\tau_g \cos\theta - A sign\dot{\theta} - B\dot{\theta} + T + \tau_h \tag{1}$$

Where (θ) joint angle, (T) exoskeleton torque, (τ_h) human torque, and (τ_g) gravitational torque of the shank/foot section are all taken into account. Inertia, solid friction coefficient, and viscous friction coefficient are represented by (J), (A), and (B), respectively.

3. PROPOSED CONTROLLER

In systems engineering, disturbance rejection is just one of several conflicting control design purposes, such as command following, robustness stabilization, noisy sensitive, and so on; in reality, however, it is frequently the design aim that design engineers are thinking about. The traditional ADRC architecture is based on the idea of using an observer, such as an extended state observer ESO, to estimate the state of the system as well as the quantity of a complete perturbation occurring on the system at the same time [26]. ADRC is a newly designed control approach aimed at gaining an insight between theory and application [10]. It will be as simple to use as a typical PID control, with additional sophisticated features such as the ability to soften set point swings using a mixture of a rapid feature synthesis and nonlinear feedback. All unknown components of the controlled system, such as unidentified disturbances and process models, are viewed by ADRC as universal disturbances, and the controller is designed to ignore them. ESO [10] is a critical component of ADRC design. Return to Eq. (1) and substitute x_1 and x_2 for the variables θ and $\dot{\theta}$. As a state variable, this equation can be formulated as follows:

$$\dot{x}_1 = x_2$$

$$\dot{x}_2 = f + b\,\tau \tag{2}$$

Where, $b = 1/J$ and f is the term for uncertainty and highly nonlinear that is combined together and is given by:

$$\frac{1}{J}\left[\tau_g \cos(x_1) - f_v\, x_2 - f_s sign(x_2) + \tau_h\right] \tag{3}$$

Rewrite Eq. (2) after added an extra state (x_3) that represent the total disturbances:

$$\dot{x}_1 = x_2$$

$$\dot{x}_2 = x_3 + b_o\,\tau \tag{4}$$

$$\dot{x}_3 = \dot{f}$$

$$y = x_1$$

The suggested observer dynamics structure of the exoskeleton modelling system in Eq. (4) is:

$$\dot{\widehat{\boldsymbol{z}}} = \boldsymbol{A}\,\widehat{z} + \boldsymbol{B}\,\tau + \boldsymbol{\beta}\,(y - \widehat{y}) \tag{5}$$

$$\widehat{y} = \boldsymbol{C}\,\widehat{\boldsymbol{z}}$$

Where, $\widehat{\boldsymbol{z}} = [\widehat{z}_1\ \widehat{z}_2\ \widehat{z}_3]^T$ is the vectors of estimates of y, $\dot{y}$, and f, respectively.

The above-mentioned observer is referred as the Linear ESO, and is referred to as the observer gain matrix. The pole-placement approach can be used to determine the components of the observer gain matrix. When properly planned and developed, the predicted observer states will match to those of the plant described by Eq. (4). The following characteristic equation can be generated using the pole-placement approach [10] and the extended state observer structure.

$$Q(s) = |s\boldsymbol{I} - (\boldsymbol{A} - \boldsymbol{\beta}\,\boldsymbol{C})| = (s + \omega_o)^3 \tag{6}$$

The observe gain matrix can be calculated using the formula below:

$$\boldsymbol{\beta} = \begin{bmatrix} 3\,\omega_o & 3\,\omega_o^2 & \omega_o^3 \end{bmatrix} \tag{7}$$

Only the bandwidth ω_o of LESO is necessary to determine the elements of the observer gain matrix. This easy tuning strategy, on the other hand, combines the performance and noise-sensitivity trade-offs. Other recent and effective optimization approaches, on the other hand, can be used to tune these parameters [19–22]. The tracking differentiator (TD) or Profile Generator (PG) is the second portion of the ADRC design, and it is used in work employing linear PG, which consists of the intended signal trajectory (r) and its derivative ($\dot{r}$). The basic goal of TD is to get around the fixed point jump constraint.

Since the PD-type control law cannot match the needs of robustness and disturbance suppression for exoskeleton system with varying disturbances, the third part of ADRC is the control law. In this paper, two controllers are used: proportional-derivative controller (PD) and sliding mod control (SMC). As a result, with payload fluctuations, the closed-loop system can achieve the desired design aim [27]. A PD-type controller is typically implemented based on the aforementioned ESO, Eq. (5) [14, 24].

$$u = \frac{\left[K_p\,(r - \widehat{z}_1) + K_d\,(\dot{r} - \widehat{z}_2) - \widehat{z}_3\right]}{b} \tag{8}$$

Let the PD controller output:-

$$u_o = K_p\,(r - \widehat{z}_1) + K_d\,(\dot{r} - \widehat{z}_2) \tag{9}$$

And rewrite Eq. (8) as:-

$$u = \frac{(u_o - \widehat{z}_3)}{b}$$

$\widehat{z}_1$ is the estimated feedback signal and $\widehat{z}_2$ is the derivative of $\widehat{z}_1$. The values of controller gains are given by $k_p = \omega_c^2$, $k_d = 2\,\omega_c$ [28, 29] where ω_c is the control loop bandwidth. In order to overcome the loss of disturbance rejection and robustness caused by the inability to fully adjust for the total disturbance f, a sliding mode term is introduced to the control law Equation (9) based on the prior arguments. Due to its resilience to external disturbances, SMC – a nonlinear control structure and well-robust control system – has been successfully applied in a wide range of engineering fields. The sliding surface is an important part of SMC since it dictates the planned state trajectories, which affects the system's stability and dynamics. The system under control is a second-order system, with the sliding surface (s) as follows:

$$s = \dot{e} + \mu e \tag{10}$$

The sliding surface coefficient (μ) is design parameter and (e) is the error, where:

$$e = r - y \tag{11}$$

The second part of SMC is the switching control:

$$U_{sw} = -Ksign(s) \tag{12}$$

The switching controller gain K is another design parameter. Substituting Eq. (10) into Eq. (12) to have

$$U_{SM} = -Ksign(\dot{e} + \mu e) \tag{13}$$

Now the control law can be included two controller parts (PD) and (SMC) so that:

$$C(s) = PD\ controller + SM\ controller$$

Eq. (9) becomes as:

$$u = \frac{(u_o - \widehat{z}_3) + U_{SM}}{b} \tag{14}$$

The tracking error derivative can be obtained. If the switching controller gain $>[f(.) + |\ddot{r}|]$, then $e\dot{e}<0$. The error will decrease to zero at a finite time. This condition for checking the stability of SMC using Lyapunov's second technique. Let derivative of Eq. (10)

$$\dot{s} = \ddot{e} + c\dot{e} \tag{15}$$

Substituting Eq. (2) and Eq. (11) into Eq. (15), and rewrite:

$$\dot{s} = \left[\ddot{r} - f(.) - bu\right] + \mu\dot{e} \tag{16}$$

or

$$\dot{s} = \hat{z}_3 - f(.) - bKsign(s) \tag{17}$$

Since $\Delta F = \hat{z}_3 - f(.)$, rewrite Eq. (17) as:

$$\dot{s} = \Delta F - K_t sign(s) \tag{18}$$

Where $K_t = bK$, the system will be stable in sense of Lyapunov if $K_t > \Delta F$ because $s\dot{s} < 0$. The sliding condition is established if $K_t > 0$. The proposed control law theorem, numerically, guarantees the operating of the system state trajectory onto sliding surface and its remaining in that position. The design parameters (K, μ) of SMC can be calculated by using PSO optimization method [15].

If one chooses the bandwidth of observer ω_o to be equal to $\omega_o = 4\,\omega_c$, then it easy to calculate the elements of observer matrix gains (β_1, β_2, β_3) according to Eq. (7). Assume that the observer gains were the same in both techniques (PD) and (SMC). Let $w_c = 24.5 rad/sec$ in the design. Figure 2 shows the structure diagram of ADRC with $C(s)$ model, which can combine the two controller techniques and $P(s)$ is the exoskeleton-human model.

4. SIMULATION RESULTS AND DISCUSSION

This part uses numerical simulations to validate the effectiveness of the designed controller. MATLAB's Simulink can be used to carry out the simulation results. Table 1 lists the

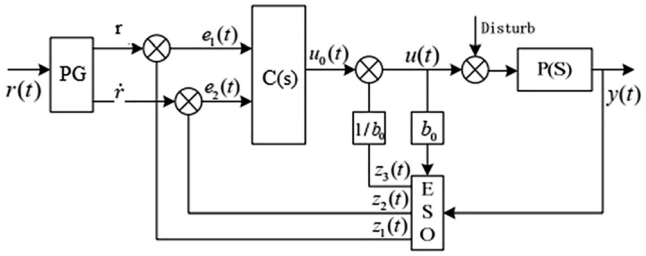

Fig. 2. Structure diagram of linear ADRC

Table 1. Shows all system variables with observer tuning parameters

Parameter	Value
Inertia (J)	0.34 $kg.\ m^2$
Solid Friction Coefficient (A)	1 $N.m$
Viscous Friction Coefficient (B)	0.9 $N.m.s./rad$
Gravity Torque (τ_g)	3.5 $N.m$
Sliding Surface Coefficient μ	0.015
Switching controller gain K	7.53
Proportional gain K_p	600
Derivative gain K_d	49
Observer gain β_1	288
Observer gain β_2	28,812
Observer gain β_3	941,192

important parameters of the human-exoskeleton system [24] as well as the control parameters.

Five categories of indices are taken into account to evaluate the performances of the controlled system in terms of error and control effort. These are the Integral of Absolute magnitude of Error (IAE), Integral Square Error (ISE), Root Mean Square Error (RMSE), Mean Absolute Error (MAE), and Integral Absolute control signal (IAU) were chosen as performance indices for comparison [9, 24, 30].To prove the advantages and superiority of the proposed SMC + PDADRC (Eq. (14)) over SMCADRC (Eq. (14) with $u_o = 0$) and PDADRC (Eq. (14) with $U_{SM} = 0$) , two cases are considered, nominal case and disturbance case. The desired trajectory angle is set as a sine curve with a frequency of 1.57 Hz and with initial condition (−0.785 rad) and moving the knee to (−1.57 rad) for full flexion and to (0 rad) for full extension in this experiment.

A Simulation Results with Nominal case

The track effectiveness of the suggested methodology is examined and compared to the SMCADRC and PDADRC approaches in the nominal case ($\tau_h = 0$) in this section. The simulation results for tracking the trajectory of the knee position and tracking error are shown in Figs 3 and 4. The proposed technique (SMC + PDADRC) responds faster than conventional controllers, resulting in lower tracking error. SMC + PDADRC compensates faster, as shown in the graph. Calculating (IAE), (ISE), (MAE), and (R.M.S.E) during the course of the tests and within 10 s, respectively, is shown in Table 2. Figure 5 depicts the control efforts required to investigate the torque (T) or $u(t)$ for three control methods. The PDADRC control method produces the least decrease in chattering in the process variable index when compared to all other controllers' approaches, according to experiment data (IAU). Because of the sign function's effect, even though SMC + PDADRC and SMCADRC response torques have higher chattering, SMC + PDADRC has less chattering than SMCARC due to the derivative effect of PD mixing with SMC, which has no effect on knee position tracking in general.

B Simulation Results with constant load disturbance case

A second simulation is run with a constant disturbance of 0.5 N.m. at time t = 2 s to test the performance of all controllers with payload condition. Figure 6 depicts the performance of the three controllers (Real vs. Desired output). Figure 7 shows the difference in knee position between the desired and actual settings for the same controllers. The SMC + PDADRC can adapt for load disturbances fast and return to the ideal trajectory in less time than the PDADRC and SMCADRC (0.35 s). When a load disturbance is added, the SMC + PDADRC technique exhibits reduced oscillation, but the PDADRC and SMCADRC methods exhibit larger oscillation while maintaining a steady tracking trajectory. Under the aforementioned simulated conditions, SMC + PDADRC is always stable and has the best tracking accuracy. As a result, the proposed method is

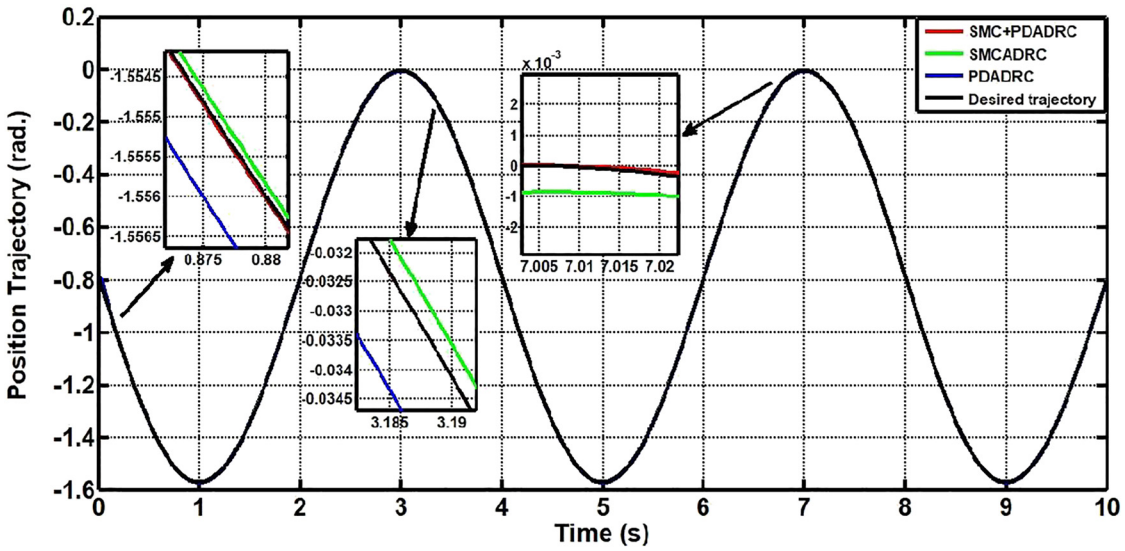

Fig. 3. The monitoring path of the knee-joint position with nominal case

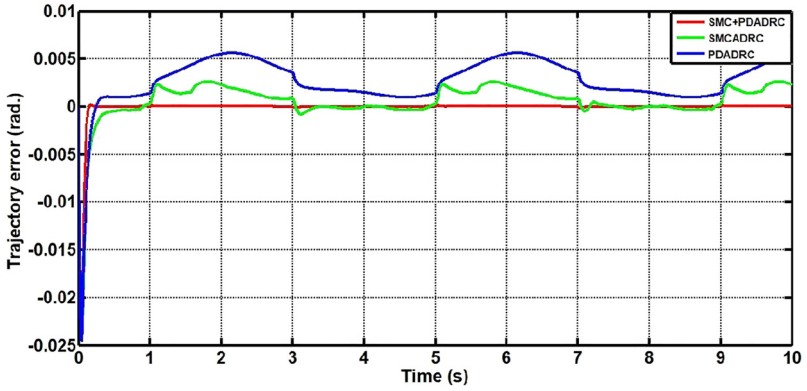

Fig. 4. Tracking error trajectories of the knee for three controllers with nominal case

Table 2. Measures of effectiveness for three controllers with nominal case

Indices	PDADRC	SMCADRC	SMC + PDADRC
R.M.S.E (rad)	0.0038	0.0023	0.0017
IAE (rad)	0.0310	0.0121	*0.0019*
ISE (rad)	0.00014	0.00005	0.00002
MAE (rad)	0.0031	0.0012	0.0001
IAU (N.m)	28.63	100	79.58

more robust to variations in load weight. Figure 8 shows the torque control efforts for three controllers. The SMCADRC and SMC + PDADRC demand more torque and have a higher index (IAU) than the PD-ADRC. Table 3 contains a list of all performance indices. The results show that as the system nears steady state, the proposed sliding gain Eq. (13) converges to near zero, preventing chattering.

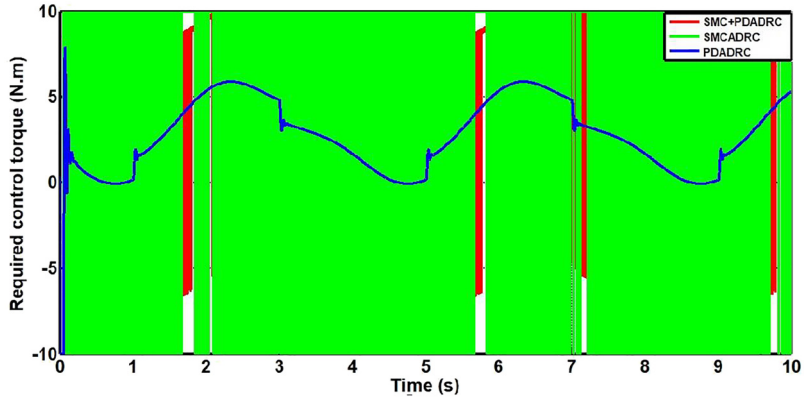

Fig. 5. Comparison of the three controllers for required torque with nominal case

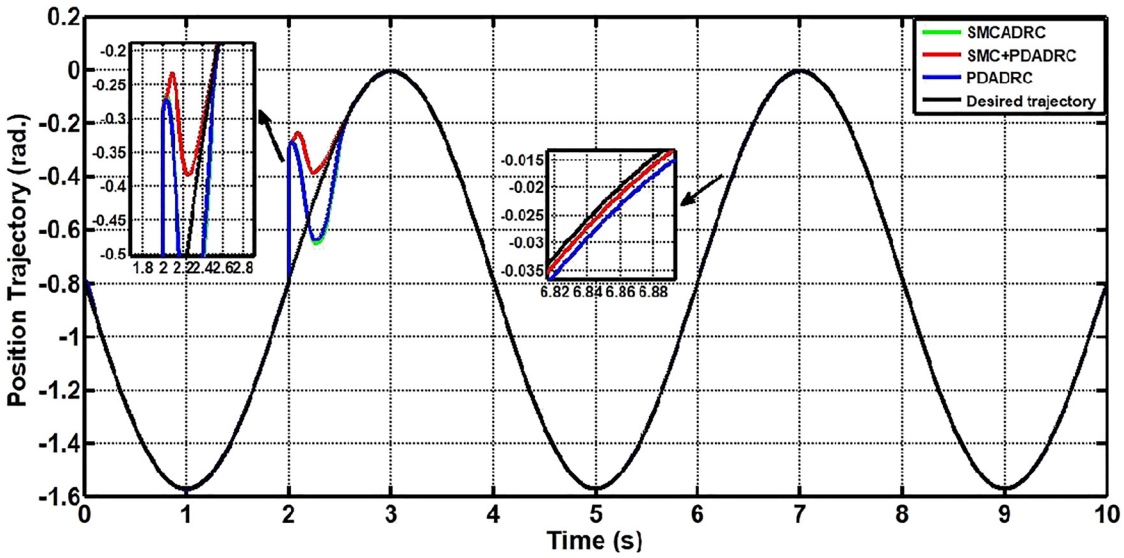

Fig. 6. The monitoring path of the knee-joint position with constant load disturbance

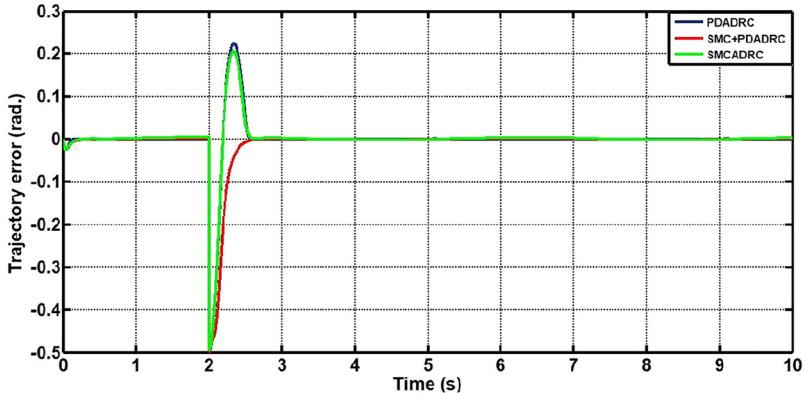

Fig. 7. Tracking error trajectories of the knee for three controllers with constant load disturbance

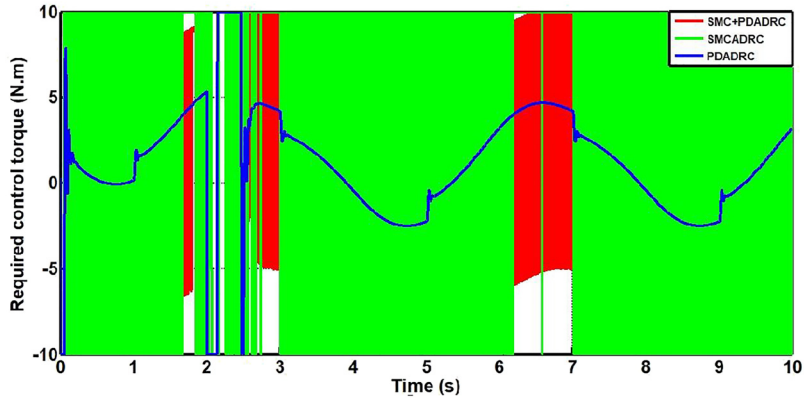

Fig. 8. Comparison of the three controllers for required torque with constant load disturbance

C Simulation Results with noise disturbance case

In fact, when a knee trajectory traveling along a pre-defined path encounters a sudden shock disturbance, such as the human effect ($\tau_h \neq 0$), another common scenario occurs. Because the knee exoskeleton may be impacted while in motion, a perturbation is added at $t = 1$ and 2 *sec*, which is a noise signal with a magnitude of ± 0.03, which is used to simulate the impact disruption in real work. Figure 9 depicts the performance of the three controllers. Figure 10 shows the

difference in knee position between the desired and actual settings for the same controllers. When compared to PDADRC and SMCDARC, which have R.M.S.E = 0.0067 and R.M.S.E = 0.0064, respectively, SMC + PDADRC can mitigate torque perturbation more quickly and, more crucially, SMC + PDADRC can drive the tracking error to converge to an acceptable range with R.M.S.E = 0.0028. Figure 11 shows the control torque efforts for three controllers. Although the SMC for both ADRC and PDADRC requires more torque and has a higher index (IAU), it can also be seen that the PDADRC requires more control signal at $t = 1$ and 2 *sec* because the variation between these limit times changes abruptly. All performance indices are listed in Table 4.

Table 3. Measures of effectiveness for three controllers with constant load disturbance case

Indices	PDADRC	SMCADRC	SMC + PDADRC
R.M.S.E (rad)	0.0584	0.0568	0.0547
IAE (rad)	0.1226	0.1111	0.1073
ISE (rad)	0.0339	0.0321	0.0298
MAE (rad)	0.0123	0.0112	0.0108
IAU (N.m)	25.11	99.94	79.17

5. CONCLUSIONS

A SMC + PDADRC approach is proposed in this paper for controlling a single knee joint rehabilitation exoskeleton. Several experiments have been conducted in the actual exoskeleton system, including angle trajectory tracking under various conditions, initially the nominal case, and then various external disturbances. The results suggest that the revised approach can track the angle of the knee joint well. The mistakes of SMC + PDADRC are greatly decreased when compared to the original PDADRC and SMCADRC in various instances, with MAE reductions of more than 69% and RMSE reductions of more than 58% in these calculations for the worst scenario (noise disturbance). The position transient can swiftly recover to normal and accomplish accurate tracking when exposed to external disturbances. In

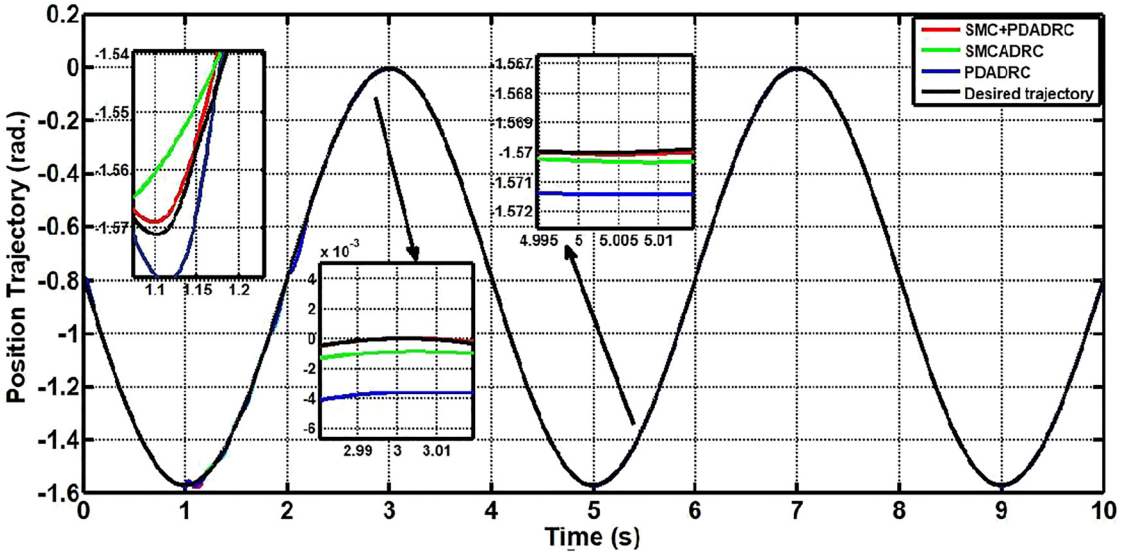

Fig. 9. The monitoring path of the knee-joint position with noise disturbance

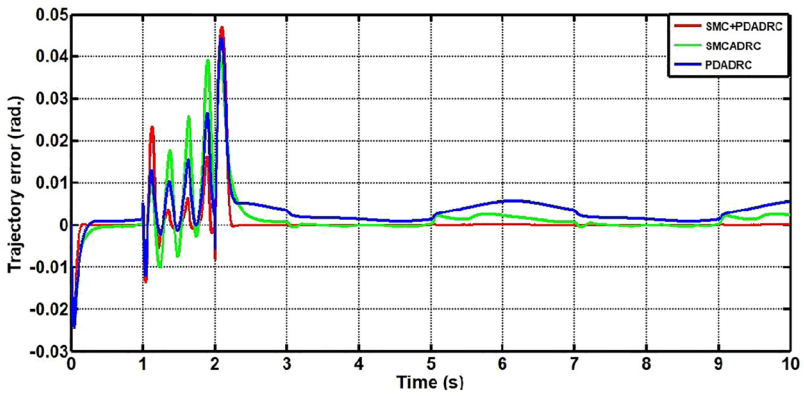

Fig. 10. Tracking error trajectories of the knee for three controllers with noise disturbance

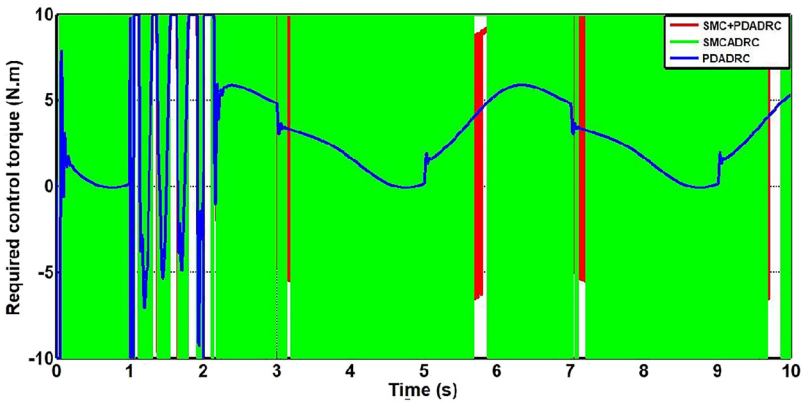

Fig. 11. Comparison of the three controllers for required torque with noise disturbance

Table 4. Measures of effectiveness for three controllers with noise disturbance case

Indices	PDADRC	SMCADRC	SMC + PDADRC
R.M.S.E (rad)	0.0067	0.0064	0.0028
IAE (rad)	0.0388	0.0276	0.0124
ISE (rad)	0.00044	0.00041	0.00030
MAE (rad)	0.0039	0.0028	0.0012
IAU (N.m)	31.92	100	80.03

general, all controller approaches demonstrate stability as measured by the error trajectory. As a result, for exoskeletons with changing payloads or disturbances, the objectives for reliability and perturbation elimination cannot be satisfied by PD-type control laws. In order to overcome the loss of disturbance rejection and robustness caused by a failure to fully adjust for the whole disturbance, a sliding mode term is introduced to the control rule. The fundamental disadvantage of SMC is chattering, which is eliminated in this study by finding the optimal coefficients of (K) and (μ). The future work is expected to include the proposed controller for 2-DOF of motion, which is applied to the Knee-Hip Exoskeleton system. Other control techniques could be suggested to conduct a comparison study for this medical application [31–34].

REFERENCES

[1] Z. A. Waheed, A. J. Humaidi, M. E. Sadiq, A. A. Al-Qassar, A. F. Hasan, A. Q. Al-Dujaili, A. R. Ajel, and S. J. Abbas, "Control of Elbow Rehabilitation System Based on Optimal-Tuned Backstepping Sliding Mode Controller," *J. Eng. Sci. Technol.*, vol. 18, no. 1, pp. 584–603, 2023.

[2] N. A. Alawad, A. J. Humaidi, A. S. Al-Araji, et al., "Improved active disturbance rejection control for the knee joint motion model," *Math. Model. Eng. Probl.*, vol. 9, no. 2, pp. 477–83, 2022.

[3] L. Zhang, G. Liu, B. Han, Z. Wang, H. Li, and Y. Jiao, "Assistive devices of human knee joint: a review," *Robot. Auton. Syst.*, vol. 25, pp. 1–31, 2020. https://doi.org/10.1016/j.robot.2019.103394.

[4] C. Xiong, X. Jiang, R. Sun, X. Huang, and Y. Xiong, "Control methods for exoskeleton rehabilitation robot driven with pneumatic muscles," *Ind. Robot Int. J.*, vol. 36, pp. 10–220, 2009. https://doi.org/10.1108/01439910910950469.

[5] Z. Wei and S. Aiguo, "Active motion control of a knee exoskeleton driven by antagonistic pneumatic muscle actuators," *Actuators*, vol. 9, pp. 1–14, 2020. https://doi.org/10.3390/act9040134.

[6] R. Baud, A. Manzoori, A. Ijspeert, et al., "Review of control strategies for lower-limb exoskeletons to assist gait," *J. Neuroengineering Rehabil.*, vol. 18, no. 119, pp. 1–34, 2021. https://doi.org/10.1186/s12984-021-00906-3.

[7] S. Shabnam and C. Silvia, "An adaptive self-organizing fuzzy logic controller in a serious game for motor impairment rehabilitation," 2017 IEEE 26th International Symposium on Industrial Electronics (ISIE), Edinburgh, UK, 2017, pp. 1311–8. https://doi.org/10.1109/ISIE.2017.8001435.

[8] C. Caulcrick, W. Huo, E. Franco, S. Mohammed, W. Hoult, and R. Vaidyanathan, "Model predictive control for human-centred lower limb robotic assistance," *IEEE Trans. Med. Robot. Bionics*, vol. 3, no. 4, pp. 980–91, Nov. 2021. https://doi.org/10.1109/TMRB.2021.3105141.

[9] W. R. Abdul-Adheem, A. T. Azar, K. I. Ibraheem, and A. J. Humaidi, "Novel active disturbance rejection control based on nested linear extended state observers," *Appl. Sci.*, vol. 10, supp. 4069, pp. 1–27, 2020. 10.3390/app10124069. https://doi.org/10.3390/app10124069.

[10] A. J. Humaidi and H. M. Badr, "Linear and nonlinear active disturbance rejection controllers for single-link flexible joint robot manipulator based on PSO tuner," *J. Eng. Sci. Technol. Rev.*, vol. 11, no. 3, pp. 133–8, 2018. 10.25103/jestr.113.18.

[11] W. R. Abdul-Adheem, I. K. Ibraheem, A. J. Humaidi, and A. T. Azar, "Model-free active input–output feedback linearization of a single-link flexible joint manipulator: an improved active disturbance rejection control approach," *Meas. Control*, vol. 54, nos 5–6, pp. 856–71, 2021. https://doi.org/10.1177/0020294020917171.

[12] E. Zhu, J. Pang, N. Sun, H. Gao, Q. Sun, and Z. Chen, "Airship horizontal trajectory tracking control based on Active Disturbance Rejection Control (ADRC)," *Nonlinear Dyn.*, vol. 75, no. 75, pp. 725–34, 2013. https://doi.org/10.1007/s11071-013-1099-x.

[13] D. Zeng, Z. Yu, L. Xiong, Z. Fu, Z. Li, P. Zhang, B. Leng, and F. Shan, "HFO-LADRC lateral motion controller for autonomous

road sweeper," *Sensors*, vol. 20, pp. 1–27, 2020. https://doi.org/10.3390/s20082274.

[14] Y. Zhao, Z. Zhao, B. Zhao, and W. Li, "Active disturbance rejection control for manipulator flexible joint with dynamic friction and uncertainties compensation," 2011 Fourth International Symposium on Computational Intelligence and Design, 2011, pp. 248–51. https://doi.org/10.1109/ISCID.2011.164.

[15] A. J. Humaidi, H. M. Badr and A. H. Hameed, "PSO-based active disturbance rejection control for position control of magnetic levitation system," in *2018 5th International Conference on Control, Decision and Information Technologies (CoDIT), Thessaloniki, Greece*, 2018, pp. 922–8. https://doi.org/10.1109/CoDIT.2018.8394955.

[16] P. Rafael, I. Lázaroab, and C. Isaac, "Adaptive sliding-mode controller of a lower limb mobile exoskeleton for active rehabilitation," *ISA Trans.*, vol. 109, no. March, pp. 218–28, 2021. https://doi.org/10.1016/j.isatra.2020.10.008.

[17] B. Mahdieh, N. Saeede, H. Mojtaba, and M. Vahid, "Sliding mode control of an exoskeleton robot for use in upper-limb rehabilitation," 2015 3rd RSI International Conference on Robotics and Mechatronics, (ICROM), 07–09 October, 2015, pp. 694–701. https://doi.org/10.1109/ICRoM.2015.7367867.

[18] L. Yi, D. Zhi-jiang, W. Wei-dong, and D. Wei, "Robust sliding mode control based on GA optimization and CMAC compensation for lower limb exoskeleton," *Appl. Bionics Biomech.*, vol. 2016, pp. 1–13, 2016. https://doi.org/10.1155/2016/5017381.

[19] B. Ibrahim, R. Ngadengon, and M. Ahmad, "Genetic algorithm optimized integral sliding mode control of a direct drive robot arm," Proceedings of the International Conference on Control, Automation and Information Sciences (ICCAIS '12), Hochi Minh City, Vietnam, November, 2012, pp. 328–33. https://doi.org/10.1109/ICCAIS.2012.6466612.

[20] F. Hassan and L. Rashad, "Particle swarm optimization for adapting fuzzy logic controller of SPWM inverter fed 3-phase IM," *Eng. Technol. J.*, vol. 29, no. 14, pp. 2912–25, 2011.

[21] A. A. Al-Qassar, A. I. Abdulkareem, A. F. Hasan, A. J. Humaidi, K. I. Ibraheem, A. T. Azar, and A. H. Hameed, "Grey-wolf optimization better enhances the dynamic performance of roll motion for tail-sitter VTOL aircraft guided and controlled by STSMC," *J. Eng. Sci. Technol.*, vol. 16, no. 3, pp. 1932–50, 2021.

[22] T. Luay, "Optimal tuning of linear quadratic regulator controller using ant colony optimization algorithm for position control of a permanent magnet dc motor," *Iraqi J. Comput. Commun. Control Syst. Eng.*, vol. 20, no. 3, pp. 29–41, 2020. https://doi.org/10.33103/uot.ijccce.20.3.3.

[23] S. Got, M. Lee, and M. Park, "Fuzzy-sliding mode control of a polishing robot based on genetic algorithm," *J. Mech. Sci. & Technol.*, vol. 15, pp. 580–91, 2001. https://doi.org/10.1007/BF03184374.

[24] N. A. Alawad, A. J. Humaidi, A. S. M. Al-Obaidi, and A. S. Alaraji, "Active disturbance rejection control of wearable lower-limb system based on reduced ESO," *Indo. J. Sci. Technol.*, vol. 7, no. 2, pp. 203–18, 2022.

[25] M. Saber and E. Djamel, "A robust control scheme based on sliding mode observer to drive a knee-exoskeleton," *Asian J. Control*, vol. 21, no. 1, pp. 439–55, 2019. https://doi.org/10.1002/asjc.1950.

[26] A. J. Humaidi, H. M. Badr and A. R. Ajil, "Design of active disturbance rejection control for single-link flexible joint robot manipulator," in *2018 22nd International Conference on System Theory, Control and Computing (ICSTCC), Sinaia, Romania*, 2018, pp. 452–7. https://doi.org/10.1109/ICSTCC.2018.8540652.

[27] W. Fan, L. Peng, J. Feng, L. Bo, P. Wei, G. Min, and X. Meilin, "Sliding mode robust active disturbance rejection control for single-link flexible arm with large payload variations," *Electronics*, vol. 10, pp. 1–15, 2021. https://doi.org/10.3390/electronics10232995.

[28] X. Chen, D. Li, Z. Gao, and C. Wang, "Tuning method for second-order active disturbance rejection control," Proceedings of the 30th Chinese Control Conference, 2011, pp. 6322–7.

[29] N. Ahmed, A. Humaidi, and A. Sabah, "Clinical trajectory control for lower knee rehabilitation using ADRC method," *J. Appl. Res. Technol.*, vol. 20, no. 5, pp. 576–83, 2022.

[30] L. Domingos, F. André, F. Dantas, d. Almeida, A. Junio, M. Edgard, "Comparison of controller's performance for a knee joint model based on functional electrical stimulation input," International IEEE/EMBS Conference on Neural Engineering (NER) Virtual Conference, May 4–6, 2021.

[31] A. J. Humaidi, S. K. Kadhim, and A. S. Gataa, "Optimal adaptive magnetic suspension control of rotary impeller for artificial heart pump," *Cybernetics and Systems*, vol. 53, no. 1, pp. 141–67, 2022. https://doi.org/10.1080/01969722.2021.2008686

[32] S. M. Mahdi, N. Q. Yousif, A. A. Oglah, M. E. Sadiq, A. J. Humaidi, and A. T. Azar, "Adaptive synergetic motion control for wearable knee-assistive system: a rehabilitation of disabled patients," *Actuators*, vol. 11, no. 7, supp. 176, pp. 1–19, 2022. https://doi.org/10.3390/act11070176.

[33] S. S. Husain, M. Q. Kadhim, A. S. M. Al-Obaidi, A. F. Hasan, A. J. Humaidi, and D. N. Al-Husaeni, "Design of robust control for vehicle steer-by-wire system," *Indo. J. Sci. Technol.*, vol. 8, no. 2, pp. 197–216, 2023.

[34] A. Al-Jodah, S. J. Abbas, A. F. Hasan, A. J. Humaidi, A. S. M. Al-Obaidi, A. A. AL-Qassar, and R. F. Hassan, "PSO-based optimized neural network PID control approach for a four wheeled omni-directional mobile robot," *Int. Rev. Appl. Sci. Eng.*, vol. 14, no. 1, pp. 58–67, 2023.